Cooperative Effect in Receptor-Mediated Endocytosis of Multiple Nanoparticles

Tongtao Yue and Xianren Zhang*

Division of Molecular and Materials Simulation, State Key Laboratory of Organic-Inorganic Composites, Beijing University of Chemical Technology, Beijing 100029, People's Republic of China

ABSTRACT

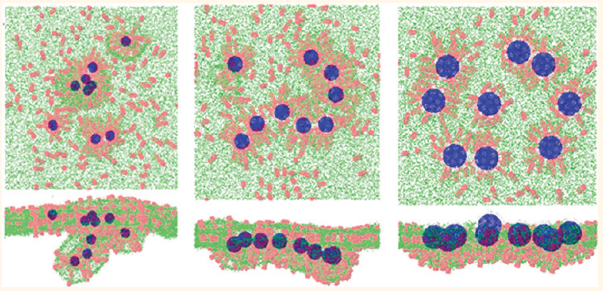

The uptake of nanoparticles (NPs) by a cellular membrane is known to be NP size dependent, but the pathway and kinetics for the endocytosis of multiple NPs still remain ambiguous. With the aid of computer simulation techniques, we show that the internalization of multiple NPs is in fact a cooperative process. The cooperative effect, which in this work is interpreted as a result of membrane curvature mediated NP interaction, is found to depend on NP size, membrane tension, and NP concentration on the membranes. While small NPs generally cluster into a close packed aggregate on the membrane and internalize, as a whole, NPs with intermediate size tend to aggregate into a linear pearl-chain-like arrangement, and large NPs are apt to separate from each other and internalize independently. The cooperative wrapping process is also affected by the size difference between neighboring NPs. Depending on the size difference of neighboring NPs and inter-NP distance, four different internalization pathways, namely, synchronous internalization, asynchronous internalization, pinocytosis-like internalization, and independent internalization, are observed.

KEYWORDS: nanoparticles · lipid membrane · aggregation · cooperative internalization · dissipative particle dynamics

In recent years, bionanotechnology has opened new avenues for clinical diagnostics and therapeutics.[1−3] In particular, nanoparticles (NPs) with different sizes, shapes, and chemical properties have been designed for drug delivery.[4,5] Therefore, understanding how NPs interact with cellular membranes is important for the design of drug nanocarriers.[6−21] In target drug delivery systems, NPs are usually functionalized with ligands,[7,10,19−23] and the specified receptor−ligand interaction enables the delivery of chemotherapy agents to targeted cells directly, which reduces side effects and leads to better patient compliance. In this case, receptor-mediated endocytosis is the main internalization pathway for NPs entering a cell.

The cellular uptake of ligand-coated NPs was found to be strongly size-dependent.[7−10,23−25] In addition, both experimental and theoretical investigations have displayed that the optimal NP size for endocytosis is on the order of 25−50 nm, while exceedingly large or small NPs would yield inefficient uptake.[6,8,10,23] Furthermore, different pathways for NP internalization, including passive and active processes, were also found to be size dependent.[9,26−28] Theoretical studies indicate that there exists one threshold particle size for the endocytosis of a single NP, below which NPs could not be encapsulated by a flexible membrane.[24] Thus, a question arises: could NPs with very small size (several nanometers) enter into cell by a mechanism of NP endocytosis when multiple NPs are taken into account? Furthermore, the mechanism of small NPs internalizing into cells or just adhering on the cell surface is still not well understood. Although biological applications of NPs require a thorough understanding of the pathway and kinetics of the uptake of multiple small NPs, to our knowledge, no quantitative study on this aspect has previously been undertaken.

Computer simulations in our previous paper show that for a single NP both the extent and dynamics of receptor-mediated endocytosis are strongly dependent on NP size, ligand density, and membrane surface tension.[29] Computer simulations also indicate that the shape anisotropy of a single NP is crucial to the nature of the interaction between the NP and cellular membrane[16] and its endocytosis.[21] However, the situation could be very different when multiple NPs are taken into account. In some cases, the multiple NPs form clusters before their adsorption on the lipid membrane, and the

* Address correspondence to zhangxr@mail.buct.edu.cn.

Received for review December 30, 2011 and accepted March 19, 2012.

Published online March 19, 2012
10.1021/nn205125e

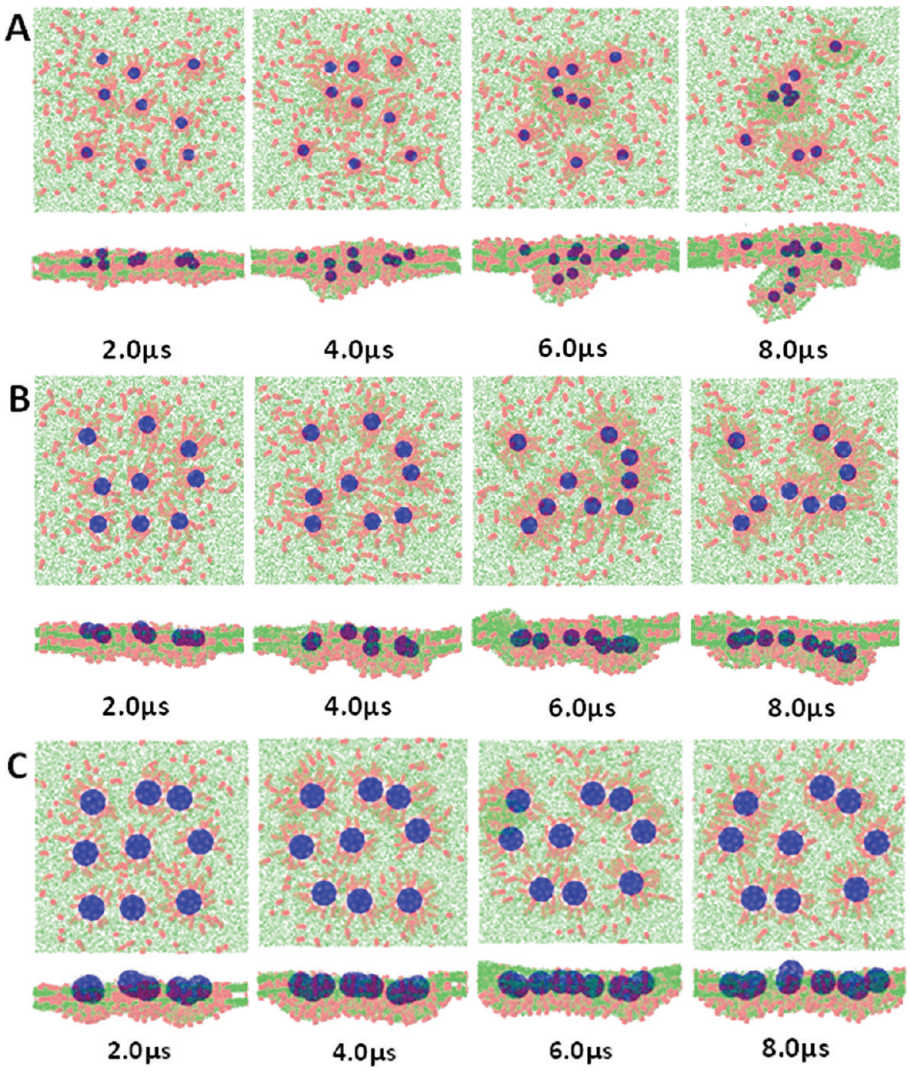

Figure 1. Typical snapshots during different internalization processes. (A) Nanoparticles with a diameter of 2.5 nm form close packed aggregates before internalization. (B) Nanoparticles having a diameter of 4.0 nm aggregate into pearl-chain-like arrangements. (C) Independent endocytosis occurs for nanoparticles having a diameter of 6.0 nm. Both top view and side view are displayed.

internalization of the NP cluster may behave as a single, large NP. In other cases, for multiple small NPs adsorbed separately on the membrane, their clustering before uptake was observed experimentally.[6,7] Experiments and computer simulations have demonstrated that curvature-inducing model proteins and NPs on lipid bilayer membranes can experience attractive interactions, and it is the attractive interactions that cause the formation of a cluster.[30−32] These works hint that the endocytosis of small NPs may occur most likely in a cooperative way.

In this work, we simulated the endocytosis of multiple NPs by a lipid membrane using a particular variant of dissipative particle dynamics (DPD), N-varied DPD.[29,33,34] With this method, the targeted membrane surface tension can be controlled by monitoring the number of lipids per area in a boundary region (for details, see the Model and Simulation Method section). Our simulations demonstrate that multiple NPs on the membrane tend to internalize into a cell cooperatively.

RESULTS AND DISCUSSION

Endocytosis of Multiple NPs Is a Size-Dependent Cooperative Process. To clarify the pathway and kinetics for the uptake of multiple NPs, nine ligand-coated NPs were placed on a large lipid membrane (51.7 nm × 51.7 nm) with 225 receptors inserted. The corresponding internalization pathway for these NPs was monitored as DPD simulation proceeds. Simulation results indicate that endocytosis of multiple NPs is a size-dependent cooperative process. Different pathways for the receptor-mediated endocytosis of multiple NPs could be observed here, depending on the NP size, NP concentration, and membrane tension.

As shown in Figure 1A, small NPs with a diameter of 2.5 nm are first partially wrapped by the membrane, and at the same time adjacent NPs gradually approach

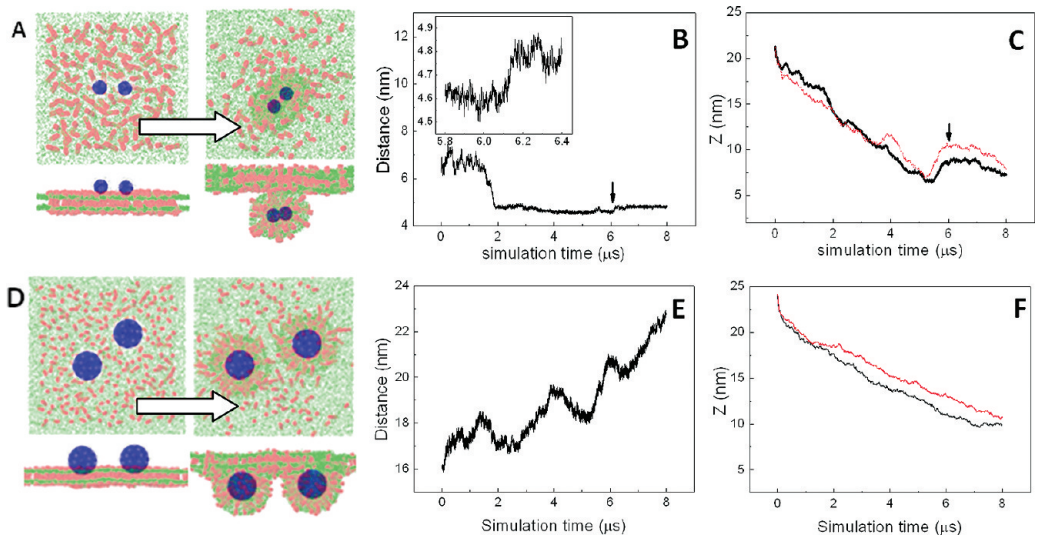

Figure 2. Endocytosis of two identical NPs. Two smaller NPs of 3.8 nm were placed on a membrane of 38.7 nm × 38.7 nm (A−C), while two larger NPs of 9.0 nm were placed on a membrane of 51.7 nm × 51.7 nm (D−F). (A, D) Initial and final structure of endocytosis of two identical NPs. (B, E) Evolution of distance between the two NPs. (C, F) Evolution of NP positions along the membrane normal direction. The initial inter-NP distances are 6.46 nm (A−C) and 15.8 nm (D−F), respectively.

each other to form a small cluster. As the simulation proceeds, the size of the cluster increases, and the cluster is encapsulated by the membrane and internalizes as a whole (see Figure 1A, and Figure S1A and Movie S1 in the Supporting Information). To show the arrangement of the lipid membrane, the configurations in Figure 1A were replotted and shown as Figure S2 in the Supporting Information. The figure clearly indicates that the lipid bilayer is not strongly perturbed by the adsorption of NPs, and the receptor density around the NPs is not high enough to form a domain in which the arrangement of lipid molecules is strongly disturbed.

For NPs with a larger size of 4.0 nm but roughly the same density of ligands, the wrapping rate becomes slower because a larger number of receptors are required to diffuse to bind the unpaired ligands coating the NPs.[7,29] Compared to the close packed aggregates formed by smaller NPs of 2.5 nm, the larger NPs tend to arrange linearly on the lipid membrane and form a pearl-chain-like structure for the subsequent endocytosis (see Figure 1B and Figure S1B). A deep groove on the lipid membrane is thus induced by the linear NP arrangement (see inset of Figure S1B). When the diameter of the NPs increases further to 6.0 nm, no obvious cooperative endocytosis is observed (see Figure 1C and Figure S1C). Contrarily, the NPs tend to be wrapped by the membrane independently. It is found that the uptake of the larger NPs becomes much slower, and the wrapping process was not complete at the end of our simulations (8 μs). We ascribe the incomplete uptake of NPs to the depletion of unpaired receptors.

Consequently, both the internalization rate and internalization pathway of multiple NPs are strongly dependent on NP size. For the internalization of a single NP, the small NP is rather difficult to wrap by a cellular membrane because significant local membrane deformation is required. For this reason, the NP of a larger size can be easily wrapped because a smaller membrane curvature is needed in the wrapping process. Nevertheless, the situation for multiple NPs is quite different, because the energy cost associated with the strong local membrane deformation to wrap a single small NP can be substantially reduced by NP clustering, which thus facilitates the wrapping process.

NP Concentration on Bilayer Membranes Affects Endocytosis Pathways. To study the effect of NP concentration in a computation cost-effective way, in this work we focused on the effect of inter-NP distance on the pathways of NP endocytosis.

We first placed two smaller NPs of 3.8 nm on a smaller lipid membrane (38.8 nm × 38.8 nm) with 121 receptors inserted and investigated how the initial inter-NP distance affects the internalization pathway. Both the final snapshots (Figure 2A) and the evolution of the inter-NP distance (Figure 2B) show that the two NPs tend to approach each other and cooperatively internalize as a whole, unless their initial distance is longer than 10.2 nm (Figure S3). We also traced the position of individual NPs along the membrane normal direction (Figure 2C), and their similar trend again confirms the existence of cooperative endocytosis. Figure 2 also shows that a slight rise of both NPs appears before the accomplishment of cooperative endocytosis (Figure 2C), which is accompanied by a slight separation between the two NPs (Figure 2B). The short period of adjustment is thought to facilitate their endocytosis.

For the cases with a larger initial inter-NP distance, the Brownian motion dominates the NP trajectories

until they are closer than a critical distance, below which they can experience the existence of their neighbors. This is why the cooperative endocytosis of two NPs with larger initial distance is more time-consuming (Figure S3F). However, if the initial inter-NP distance is larger than 10.2 nm, the NPs tend to be wrapped by the membrane independently with a much longer internalization time (Figure S3G, H).

We also placed two large NPs (D = 9.0 nm) on a larger membrane (51.7 nm × 51.7 nm) and explored the effect of initial inter-NP distance on the wrapping process. We found that the two NPs tend to internalize independently (Figure 2D–F) unless they initially contact each other (Figure S4). In this case, the curvature energy of the membrane is reduced as the NP diameter increases, and the strong receptor–ligand interaction exceeds the energy cost to bend a membrane. Therefore, to maximize the number of receptor–ligand interactions, the NPs prefer to depart from each other, rather than approach each other to minimize the membrane bending.

Membrane Curvature Mediated NP Interaction. In this work, the clustering of NPs without direct attraction in Figure 1 is ascribed to the membrane curvature mediated attraction.[31,32] The effective attraction between neighboring NPs arises purely as a result of membrane curvature induced by NP adsorption. Due to the strong receptor–ligand interaction, the local geometry of a small NP deforms the membrane and produces a local membrane curvature. When two membrane-curving NPs approach each other, the bilayer deformations overlap. Then neighboring NPs might cluster in order to reduce the curvature energy of the membrane because the clustering could share the work needed to bend the membrane and thereby lower the stored elastic energy.[24] The curvature-mediated interaction between small NPs is thus effectively attractive even through without direct attraction between neighboring NPs.

The membrane curvature mediated interaction between neighboring NPs is found to be strongly sensitive to NP size (see Figures 1 and Figure 2). For example, increasing the NP size would weaken the membrane curvature mediated interaction because the increase of the NP size lowers the local membrane curvature. Moreover, when the NP size becomes large enough, we found that the effective interaction between neighboring NPs seems to be repulsive, as shown in Figure 1C and Figure 2D–F. This is because in this case the strong receptor–ligand interaction exceeds the energy cost to bend a membrane. Therefore, to maximize the number of receptor–ligand interactions, the NPs tend to internalize separately, rather than aggregate to share the unfavorable membrane curvature. In general, not only the strength but also the sign of the membrane curvature mediated interaction between neighboring NPs is strongly sensitive to the NPs' size.

Besides the NP size, the initial inter-NP distance or equivalently the dose of NPs also affects the membrane curvature mediated interaction and, therefore, the internalization pathway. For small NPs, they experience no attraction until they approach a critical distance below which the NP-induced bilayer deformations overlap, while for NPs of intermediate size, once they are partially wrapped by the membrane, the longer range interaction connects them one by one to form a linear arrangement (see Figure 1B and movie S2). In general, it is the curvature-mediated attraction, which varies with NP size, NP distance, and the wrapping extent (membrane curvature), that determines the NP arrangement and the subsequent internalization rate. This explains why different internalization pathways occur for NPs of different sizes. For example, this explains why a pearl-chain-like arrangement or even separate endocytosis occurs for larger NPs: the membrane curvature mediated attraction gradually becomes repulsive as the NP size increases.

Note that there exists another possible explanation for the clustering of NPs, *i.e.*, the coalescence of small domains, which reduces the free energy of the domain boundaries. The mechanism of domain coarsening was used to interpret the budding dynamics of multicomponent membranes.[35] In this work, however, we confirm that it is the surface curvature of NPs causing the interaction between neighboring NPs, rather than the coarsening of domains formed as the result of the enrichment of receptor molecules surrounding the NPs. We placed two disk-like NPs on the membrane surface and monitored their interaction. Snapshots (Figure S5A–C in the Supporting Information) and the evolution of NP distance (Figure S5D–F) indicate that there is no obvious tendency for two disk-like NPs to cluster. Therefore, the clustering of NPs and the cooperative internalization are mainly induced by the curvature-mediated interaction.

Membrane Tension Affects Endocytosis Pathways. To explore the effect of membrane tension on the internalization of multiple NPs, we placed two NPs on membranes with different membrane tensions. We found that especially for smaller NPs the negative membrane tension is a prerequisite for their internalization.

When the membrane tension is highly negative, two small NPs are usually wrapped by the membrane cooperatively (Figure 3A–C). As the membrane tension increases gradually, the wrapping rate decreases due to the increase of energy cost to bend a membrane (Figure 3D, E). However, when two NPs are placed on a membrane with nearly zero tension, these two NPs stay slightly wrapped by the membrane in our simulation and no NP internalization occurs (Figure 3G, I). In this case, due to the small membrane bending, the curvature-mediated attraction becomes so weak that it could not drive the two NPs to cluster (Figure 3H). In addition, the strong energy cost for membrane bending prevents the

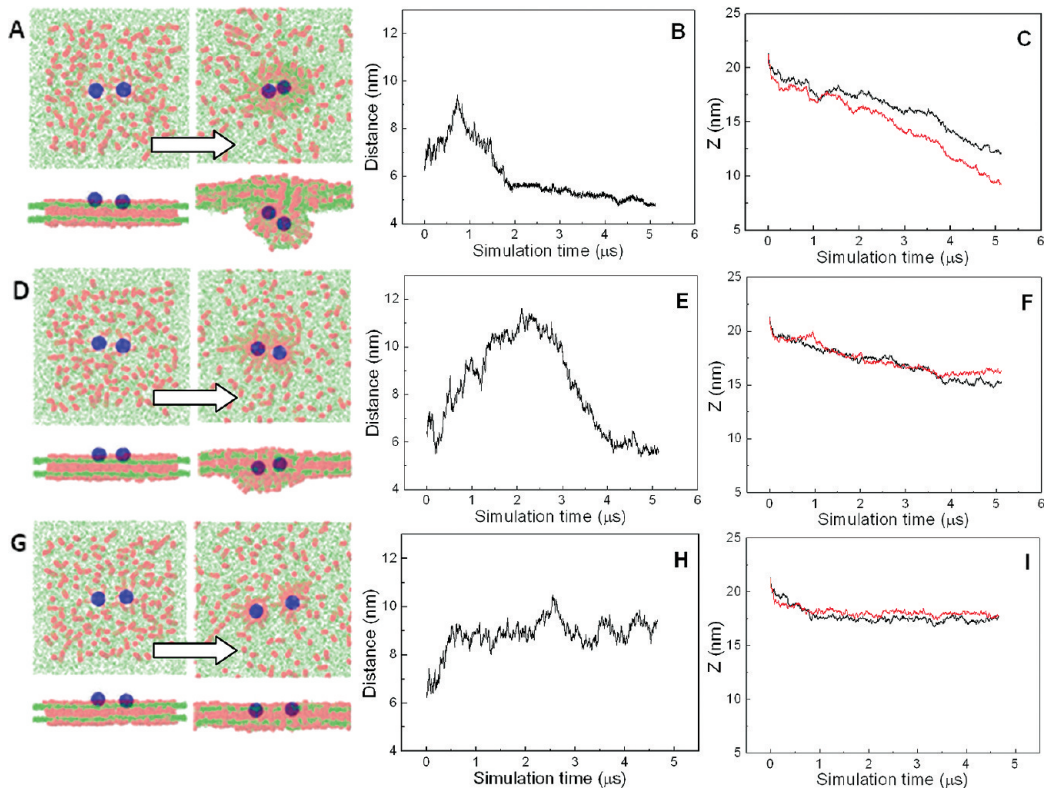

Figure 3. Internalization of two small NPs (3.8 nm) on the membrane with different surface tension. (A–C) 1.59 < ρ_{LNPA} < 1.63; (D–F) 1.53 < ρ_{LNPA} < 1.57; (G–I) 1.48 < ρ_{LNPA} < 1.52. (A, D, G) Initial and final structure of endocytosis of two identical NPs. (B, E, H) Evolution of distance between two NPs. (C, F, I) Evolution of NP positions along the membrane normal direction.

NP internalization individually. Therefore, a negative membrane tension is necessary to induce the cooperative internalization of small NPs. As the membrane tension increases, the cooperative effect disappears and the internalization of small NPs becomes impossible.

Receptor–Ligand Interaction Affects Internalization Efficiency. We note that the real receptor–ligand interactions in nature are anisotropic, and this anisotropic interaction can affect the binding geometry to some extent. However, in order to simplify the question and reduce the computational cost, we employed coarse-grained models for both ligands and receptors and the anisotropy of the receptor–ligand interaction is ignored.

To investigate the effect of receptor–ligand interaction parameter a_{LR_H} on the NP internalization, we varied a_{LR_H} from 0.0 to as large as 22.0, and the internalization processes for two identical NPs of 3.8 nm were simulated. The final configurations at ~5 μs (Figure S6A in the Supporting Information) show that the two NPs can be internalized cooperatively as long as a_{LR_H} is not larger than 22.0. The evolution of the number of ligands bound to receptors (Figure S6B–D) also demonstrates that the rate of NP wrapping decreases slightly as the receptor–ligand binding energy decreases. Therefore, the efficiency of NP wrapping is affected by the receptor–ligand interaction strength.

Size Difference between NPs Affects Endocytosis Pathways. On the basis of the above analysis, both NP size and inter-NP distance (NP concentration or dose) are essential for the pathway of NP internalization. However, it is noteworthy that in the fabrication of NPs for their practical applications, such as drug delivery materials, it is hard to control the size of NPs strictly. Therefore, exploring the effect of the size difference between neighboring NPs on the internalization pathway becomes quite important.

To study this effect, in this work two NPs with different sizes were placed on a lipid membrane, and their internalization pathways were then monitored from DPD simulations. In the simulation runs, the diameter of the larger NP was fixed to 4.5 nm, and that of the other increases from 2.5 nm, to 3.3 nm, to 4.0 nm.

According to the final structures (Figure 4A–C), the evolution of inter-NP distance (see inset of Figure 4D–F), and NP positions along the *z* axis (Figure 4D–F), one can conclude that the internalization of two NPs with different sizes is a cooperative process. Nevertheless, their internalization pathway is strongly affected by the size difference. The cooperative effect becomes weakened as the size difference increases, which is clearly revealed by the gradual increase of the inconsistency for the two NPs in their position evolution along the *z* axis (Figure 4D–F). The final structures in Figure 4A reveal that when the size difference between the two

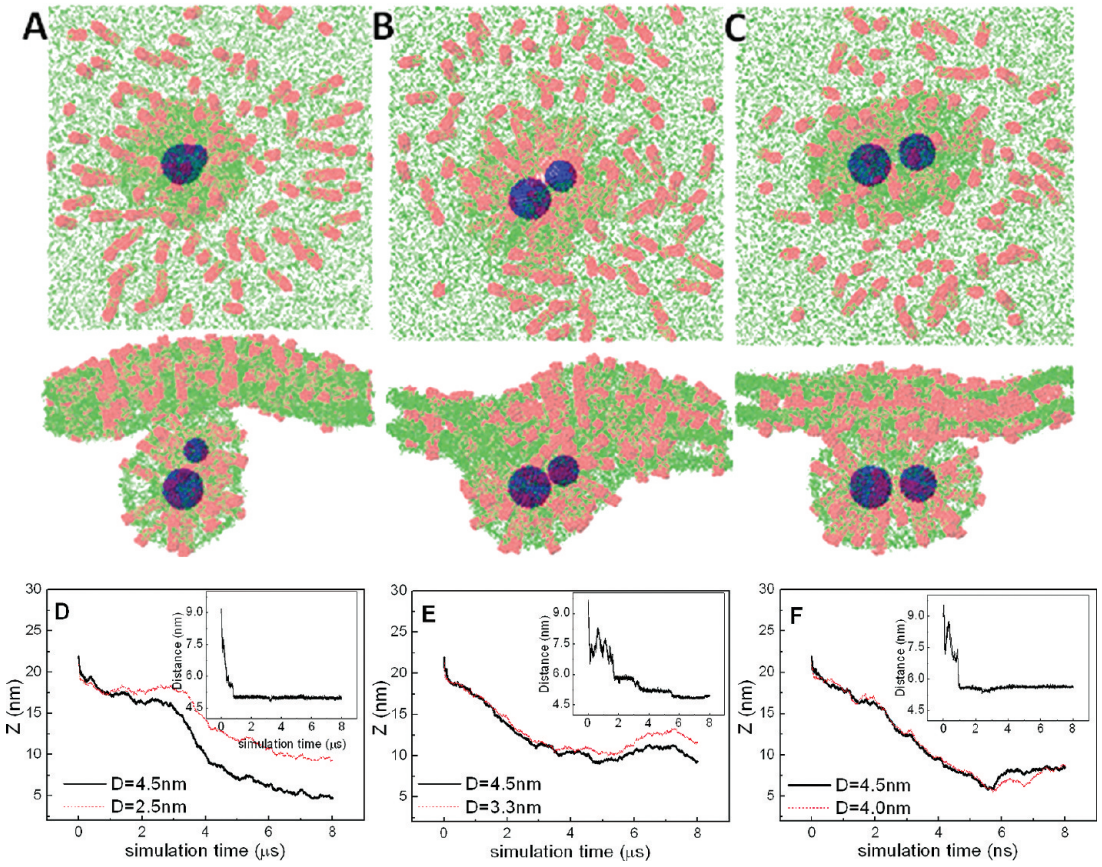

Figure 4. Cooperative endocytosis of two NPs of different size. (A–C) Typical snapshots showing different internalization pathways. (D–F) NP position along the membrane normal, in which the evolution of the inter-NP distance is also given (inset).

NPs is noticeable (*e.g.*, one is 4.5 nm and the other is 2.5 nm), the larger NP tends to internalize first due to its smaller curvature, which is followed by the uptake of the smaller one. This one-by-one internalization pathway, which is called asynchronous internalization here, is then weakened by decreasing the size difference (Figure 4B). When the diameter of the smaller NP increases to 4.0 nm, the two NPs are internalized almost simultaneously (Figure 4C). In this case, the internalization pathway is called synchronous internalization.

Independent simulation runs indicate that there exist different internalization pathways even for the same system. By using the first situation (the diameters for the two NPs are 4.5 and 2.5 nm, respectively) as an example, 10 independent simulations were performed under the same conditions. Five of these simulations show that the NPs internalize in a one-by-one manner. In the other simulation runs, however, three of them indicate that the NPs internalize *via* a pinocytosis-like pathway (Figure 5), and the others show an independent internalization (Figure 6).

We first concentrate on the pinocytosis-like internalization (Figure 5). In the initial stage, two NPs are both slightly wrapped by the lipid membrane due to the receptor–ligand interactions. As the simulation proceeds, the distribution of receptors around the larger NP becomes no longer uniform due to the existence of the smaller NP. Besides, the smaller NP and the receptors that it bound together rigidify the local membrane region near the larger NP. Consequently, the membrane wrapping from the side of the smaller NP is restricted. As a result, the membrane has to protrude from the other side to wrap the larger NP. This protrusion continuously grows, and the membrane finally wraps the larger NP from the top side, just like in pinocytosis (Figure 5). The evolution of the extent of wrapping (Figure 5B), inter-NP distance (see inset of Figure 5C), and NP positions along the *z* axis (Figure 5C) all indicate that the pinocytosis-like internalization is a cooperative wrapping process. Here, we must note that a negative membrane tension is a prerequisite for the occurrence of pinocytosis-like endocytosis. The other factors affecting the pinocytosis-like endocytosis are the size difference and the initial distance between two neighboring NPs, which will be discussed below.

The simulation runs also demonstrate that there exists an internalization pathway without a cooperative effect involved. Typical snapshots (Figure 6A) and time evolution of the extent of wrapping (Figure 6B) show that the larger NP is wrapped by the membrane and internalized gradually, while the smaller NP stays

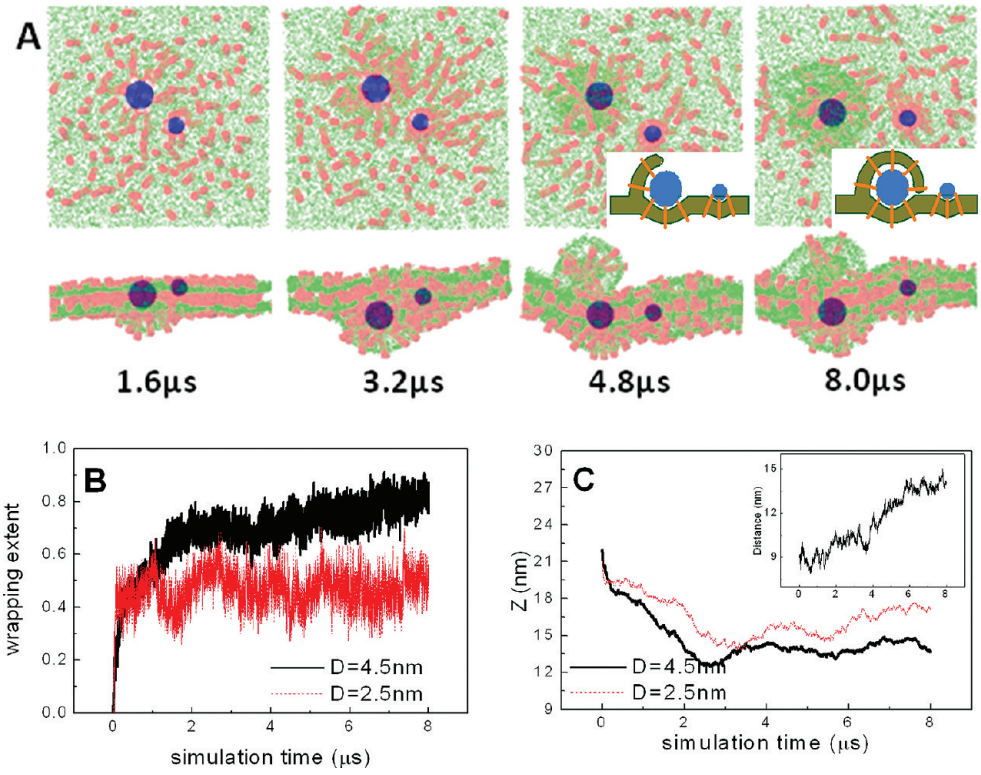

Figure 5. Pinocytosis-like internalization pathway for two NPs of different size. (A) Typical snapshot during the pinocytosis-like internalization process. (B) Evolution of the wrapping extent for the two NPs. (C) NP positions along the membrane normal direction, in which the evolution of the inter-NP distance is also given (inset).

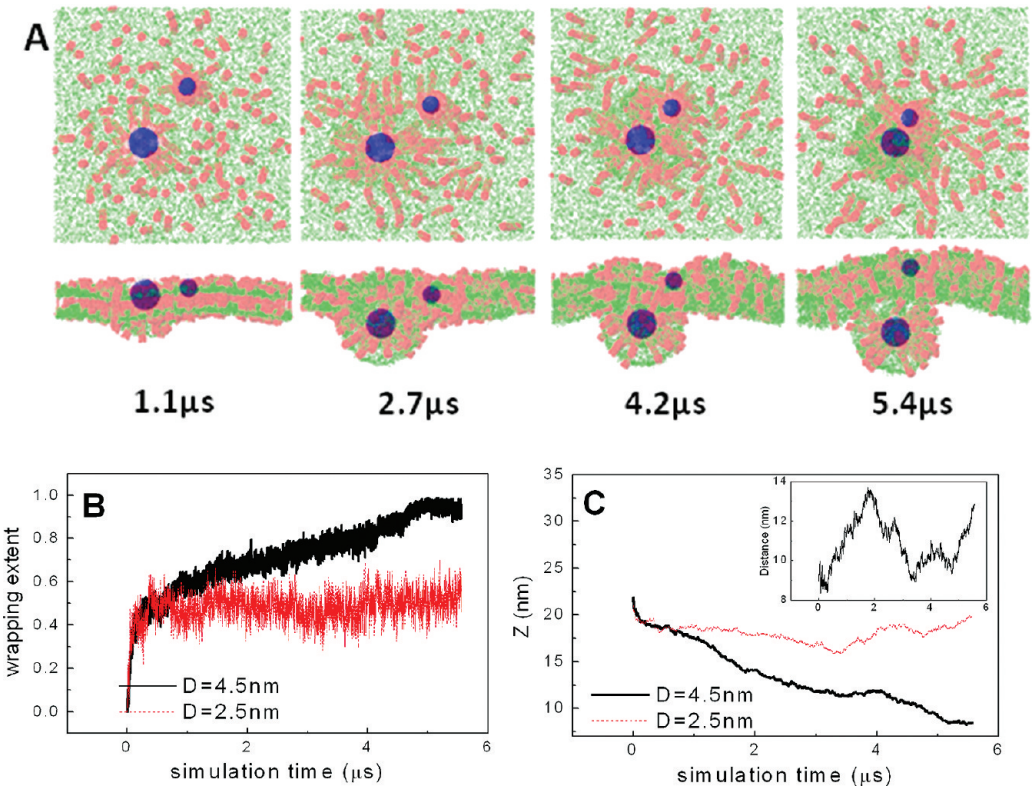

Figure 6. Independent internalization pathway for two NPs of different sizes. (A) Typical snapshot during the independent internalization process. (B) Evolution of the wrapping extent for the two NPs. (C) NP positions along the membrane normal direction, in which the evolution of the inter-NP distance is also given (inset).

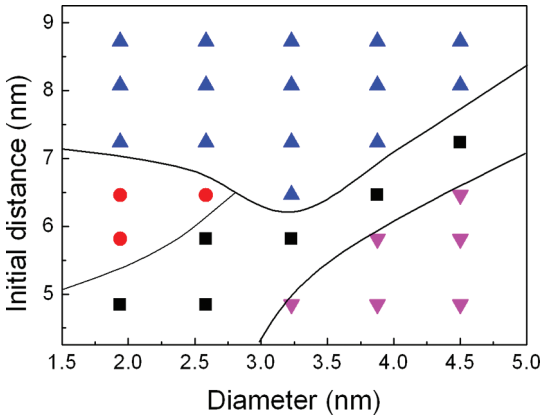

Figure 7. Internalization pathway for two neighboring NPs as functions of the NP size and the initial inter-NP distance. ▲ represents the independent internalization pathway; ● represents the pinocytosis-like internalization pathway; ■ represents asynchronous internalization; and ▼ represents synchronous internalization. Note that the diameter of the larger NP is fixed to 4.5 nm.

adhered on the membrane surface. This observation is further confirmed by the evolution of NP positions along the *z* axis (Figure 6C). Furthermore, the alternative increase and decrease of NP distances (see inset of Figure 6C) indicates that the cooperative effect plays a negligible role in the internalization process, which is different from those in processes of pinocytosis-like internalization (see inset of Figure 5C) and cooperative internalization (synchronous and asynchronous internalization in Figure 4).

In order to understand the effect of NP size difference and initial inter-NP distance on their internalization pathway systematically, we varied the size of the smaller NP and their initial distance while fixing the larger NP size to 4.5 nm. As shown in Figure 7, four different internalization pathways are observed: independent internalization, pinocytosis-like internalization, synchronous internalization, and asynchronous internalization, respectively.

In general, when two NPs are well separated, they tend to be wrapped by the lipid membrane independently. As the inter-NP distance gradually decreases, other types of internalization processes are observed. The pinocytosis-like internalization takes place for two NPs having a large size difference and moderate inter-NP distance. Synchronous internalization, however, tends to occur for two NPs with similar size but at shorter initial distance. In contrast, the asynchronous internalization can be observed when the two NPs have a large or small size difference, but the initial inter-NP distance required for asynchronous internalization increases as their size difference increases.

In our simulations, the internalization of NPs can be considered as the result of competition between the thermodynamic driving force due to the receptor–ligand binding and the energy cost to bend a membrane. The driving force is mainly determined by the receptor (ligand) density and receptor–ligand binding energy, while the membrane bending energy is determined by the membrane tension and NP size (curvature).

Therefore, when two NPs of different size are placed on a lipid membrane, the larger NP always tends to internalize first, while the internalization of a smaller NP is relatively difficult because of the higher curvature. Because local membrane rigidity can be strengthened by the existence of receptors and neighboring NPs, the internalization pathway of the larger NP is strongly affected by the existence of a smaller NP and the receptor–ligand binding. When the smaller NP is close to the larger NP, it can be wrapped by the membrane together with the larger NP (Figure 4A). However, increasing the inter-NP distance may induce the occurrence of pinocytosis-like (Figure 5) and independent internalization (Figure 6). In general, the internalization of two NPs is strongly determined by the NP size difference and the inter-NP distance.

CONCLUSIONS

The uptake of nanoparticles by cellular membranes is known to be NP size dependent, but the pathway and kinetics for the endocytosis of multiple NPs still remain ambiguous. In this work, we have used the DPD simulation method to show that the internalization of multiple NPs is in fact a cooperative process. This is because the energy cost associated with the strong local membrane deformation to wrap a single small NP can be minimized by NP clustering, which hence further facilitates the wrapping process.

The cooperative effect, which is caused by membrane curvature mediated NP attraction, depends on NP size, membrane tension, and NP concentration on the membranes. The membrane curvature mediated attraction between neighboring NPs arises purely as a result of membrane curvature induced by NP adsorption. The local geometry of adsorbed NPs deforms the membrane and produces a local membrane curvature. Thus neighboring NPs might cluster in order to reduce the curvature energy of the membrane because the clustering could share the work needed to bend the membrane and thereby lower the stored elastic energy.

The membrane-mediated interaction between neighboring NPs is found to be strongly sensitive to NP size. Increasing the NP size would weaken the membrane curvature mediated interaction because increasing the NP size lowers the perturbation of the membrane curvature. Moreover, when the NP size becomes large enough, the effective interaction between neighboring NPs may become repulsive, because in this case the strong receptor–ligand interaction exceeds the energy cost to bend a membrane. As a result, small NPs are found to cluster into a close packed aggregate on

the membrane and internalize as a whole. While NPs with intermediate size tend to aggregate into a pearl-chain-like arrangement, large NPs are apt to separate from each other and internalize independently.

Besides the NPs size, the inter-NP distance or equivalently the dose of NPs also affects the membrane curvature mediated interaction and thus affects the NP arrangement and the subsequent internalization pathways. The NPs with an initial inter-NP distance shorter than a critical value tend to approach each other and cooperatively internalize as a whole. However, if the initial inter-NP distance is larger than the critical value, the NPs tend to be wrapped by the membrane independently.

We also explored the effect of membrane tension on the internalization of multiple NPs. We found that, especially for smaller NPs, the negative membrane tension is a prerequisite for their internalization. As the membrane tension increases, the cooperative effect disappears and the internalization of small NPs becomes impossible.

A cooperative wrapping process is also affected by the size difference between neighboring NPs. Depending on the size difference and inter-NP distance, four different internalization pathways, namely, synchronous internalization, asynchronous internalization, pinocytosis-like internalization, and independent internalization, are observed.

MODEL AND SIMULATION METHOD

Model. In this system, a model lipid[29,34,36−38] is constructed by connecting a headgroup with three hydrophilic beads (H) to two hydrophobic tails of equal length, each having five hydrophobic beads (T). This lipid model represents dimyristoylphosphatidylcholine and was found to form stable bilayers and show typical phase behavior of the lipid bilayers.[39,40] The transmembrane receptor embedded in the lipid bilayer membranes is modeled by linking seven amphipathic chains into a cylindrical bundle. Each amphipathic chain is composed of six hydrophobic beads (R_T), each end connecting three hydrophilic beads (R_H). The seven amphipathic chains are linked to their neighbors by a spring-like interaction, thus forming a relatively rigid body without evident internal flexibility. The spherical solid nanoparticle, which is composed of solid beads (P) with a number density of 3, is constrained to move as a rigid body. Solvent molecules (W) and other beads are not allowed to enter the interior of the NPs. The ligands (L) coating the surface of the NPs are modeled as short cylindrical rods.

The dissipative particle dynamics method was first introduced to simulate the hydrodynamic behavior of complex fluids[41−43] and proved to be especially useful in studying the mesoscale behaviors of lipid membranes.[36,44,45] The elementary units of DPD simulations are soft beads whose dynamics are governed by Newton's equation of motion, similar to the molecular dynamics method. The interbead force exerted on each bead is composed of conservative, dissipative, and random forces. In this system, the interaction parameters between beads of the same type were set to $a_{WW} = a_{HH} = 25$ and $a_{TT} = 15$, and those between the different types of beads were $a_{TW} = a_{R_TW} = 80$, $a_{HT} = a_{R_HT} = a_{R_TH} = a_{R_HR_T} = 50$, $a_{HW} = a_{R_HW} = 25$, and $a_{TR_T} = 15$. Specifically, in order to avoid aggregation of the transmembrane receptors, the interaction parameters were set to $a_{R_HR_H} = a_{R_TR_T} = 50$. To describe the strong binding interaction between ligands and mobile receptors, the receptor−ligand interaction parameter is set to $a_{LR_H} = 0.0$ unless otherwise specified. Furthermore, the NPs and ligands are thought to be hydrophobic, and thus their interactions with solvent were set to $a_{PW} = a_{LW} = 80$. Although some atomistic details were sacrificed during this coarse-graining procedure, the essential features of the system are reproduced by the simulation model and the parameter set. In the model of lipids and proteins, the interaction between neighboring beads along the same molecules and the force containing the variation of bond angles were given in our previous work.[29]

N-Varied DPD Simulation Method. In this work, we used the N-varied DPD simulation method,[29,33,34] a particular variant of the DPD method in which the targeted membrane surface tension can be controlled by monitoring the number of lipids per area (LNPA) in a boundary region. The boundary region of the membrane, which surrounds the central square region of the membrane, plays a role as a reservoir of lipids. The value of LNPA in the boundary region is kept in a defined range ($\rho_{LNPA}^{min} < \rho_{LNPA} < \rho_{LNPA}^{max}$) by addition/deletion moves of the lipids. In an addition move, new lipid molecules are inserted into the boundary region if the local lipid area density is less than ρ_{LNPA}^{min}. Conversely, if the average area density of lipids in the boundary region exceeds ρ_{LNPA}^{max}, a few lipid molecules should be deleted randomly from the boundary region. Simultaneously, a corresponding number of water beads is randomly added or deleted to keep the whole density of the beads in the simulation box constant. In practice, we performed one addition/deletion move every 1500 time steps in order to leave enough time to propagate the membrane tension to the whole membrane.

Conflict of Interest: The authors declare no competing financial interest.

Acknowledgment. The authors thank the "Chemical Grid Project" of BUCT for the generous allocations of computer time and excellent technical assistance. This work was financially supported by National Natural Science Foundation of China (No. 20736005 and No. 20876004).

Supporting Information Available: Additional simulation results and videos. These materials are available free of charge *via* the Internet at http://pubs.acs.org.

REFERENCES AND NOTES

1. Cao, Y. W. C.; Jin, R. C.; Mirkin, C. A. Nanoparticles with Roman Spectroscopic Fingerprints for DNA and RNA Detection. *Science* **2002**, *297*, 1536–1540.
2. Bechet, D.; Couleaud, P.; Frochot, C.; Viriot, M. L.; Guillemin, F.; Barberi-Heyob, M. Nanoparticles as Vehicles for Delivery of Photodynamic Therapy Agents. *Cell* **2008**, *26*, 612–621.
3. Lopez, C. F.; Nielsen, S. O.; Moore, P. B.; Klein, M. L. Understanding Nature's Design for a Nanosyringe. *Proc. Natl. Acad. Sci. U. S. A.* **2004**, *101*, 4431–4434.
4. Hughes, G. A. Nanostructure-Mediated Drug Delivery. *Nanomedicine* **2005**, *1*, 22–30.
5. Kohane, D. S. Microparticles and Nanoparticles for Drug Delivery. *Biotechnol. Bioeng.* **2007**, *96*, 203–209.
6. Chithrani, B. D.; Ghazani, A. A.; Chan, W. C. W. Determining the Size and Shape Dependence of Gold Nanoparticle Uptake into Mammalian Cells. *Nano Lett.* **2006**, *6*, 662–668.
7. Chithrani, B. D.; Chan, W. C. W. Elucidating the Mechanism of Cellular Uptake and Removal of Protein-Coated Gold Nanoparticles of Different Sizes and Shapes. *Nano Lett.* **2007**, *7*, 1542–1550.
8. Jiang, W.; Kim, B. Y. S.; Rutka, J. T.; Chan, W. C. W. Nanoparticle-Mediated Cellular Response Is Size-Dependent. *Nat. Nanotechnol.* **2008**, *3*, 145–150.
9. Gratton, S. E. A.; Ropp, P. A.; Pohlhaus, P. D.; Luft, J. C.; Madden, V. J.; Napier, M. E.; DeSimone, J. M. The Effect of

Particle Design on Cellular Internalization Pathways. *Proc. Natl. Acad. Sci. U. S. A.* **2008**, *105*, 11613–11618.
10. Zhang, S. L.; Li, J.; Lykotrafitis, G.; Bao, G.; Suresh, S. Size-Dependent Endocytosis of Nanoparticles. *Adv. Mater.* **2009**, *21*, 419–424.
11. Roiter, Y.; Ornatska, M.; Rammohan, A. R.; Balakrishnan, J.; Heine, D. R.; Minko, S. Interaction of Nanoparticles with Lipid Membrane. *Nano Lett.* **2008**, *8*, 941–944.
12. Cho, E. C.; Xie, J. W.; Wurm, P. A.; Xia, Y. N. Understanding the Role of Surface Charges in Cellular Adsorption *versus* Internalization by Selectively Removing Gold Nanoparticles on the Cell Surface with a I_2/KI Etchant. *Nano Lett.* **2009**, *9*, 1080–1084.
13. Lin, J. Q.; Zhang, H. W.; Chen, Z.; Zheng, Y. G. Penetration of Lipid Membranes by Gold Nanoparticles: Insights into Cellular Uptake, Cytotoxicity, and their Relationship. *ACS Nano* **2010**, *4*, 5421–5429.
14. Wong-Ekkabut, J.; Baoukina, S.; Triampo, W.; Tang, I. M.; Tieleman, D. P.; Monticelli, L. Computer Simulation Study of Fullerene Translocation through Lipid Membranes. *Nat. Nanotechnol.* **2008**, *3*, 363–368.
15. Wallace, E. J.; Sansom, M. S. P. Blocking of Carbon Nanotube Based Nanoinjectors by Lipid: A Simulation Study. *Nano Lett.* **2008**, *8*, 2751–2756.
16. Yang, K.; Ma, Y. Q. Computer Simulation of the Translocation of Nanoparticles with Different Shapes across a Lipid Bilayer. *Nat. Nanotechol.* **2010**, *5*, 579–583.
17. Nel, A. E.; Mädler, L.; Velegol, D.; Xia, T.; Hoek, E. M. V.; Somasundaran, P.; Klaessig, F.; Castranova, V.; Thompson, M. Understanding Biophysicochemical Interactions at the Nano-Bio Interface. *Nat. Mater.* **2009**, *8*, 543–557.
18. Alexeev, A.; Uspal, W. E.; Balazs, A. C. Harnessing Janus Nanoparticles to Create Controllable Pores in Membranes. *ACS Nano* **2008**, *2*, 1117–1122.
19. Verma, A.; Uzun, O.; Hu, Y. H.; Hu, Y.; Han, H. S.; Watson, N.; Chen, S.; Irvine, D. J.; Stellacci, F. Surface-Structure-Regulated Cell-Membrane Penetration by Monolayer-Protected Nanoparticles. *Nat. Mater.* **2008**, *7*, 588–596.
20. Shi, X. H.; Bussche, A.; Hurt, R. H.; Kane, A. B.; Gao, H. J. Cell Entry of One-Dimensional Nanomaterials Occurs by Tip Recognition and Rotation. *Nat. Nanotechnol.* **2011**, *6*, 714–719.
21. Vácha, R.; Martinez-Veracoechea, F. J.; Frenkel, D. Receptor-Mediated Endocytosis of Nanoparticles of Various Shapes. *Nano Lett.* **2011**, *11*, 5391–5395.
22. Verma, A.; Stellacci, F. Effect of Surface Properties on Nanoparticle-Cell Interactions. *Small* **2010**, *6*, 12–21.
23. Gao, H. J.; Shi, W. D.; Freund, L. B. Mechanics of Receptor-Mediated Endocytosis. *Proc. Natl. Acad. Sci. U. S. A.* **2005**, *102*, 9469–9474.
24. Lipowsky, R.; Döbereiner, H.-G. Vesicles in Contact with Nanoparticles and Colloids. *Europhys. Lett.* **1998**, *43*, 219–225.
25. Smith, K. A.; Jasnow, D.; Balazs, A. C. Designing Synthetic Vesicles that Engulf Nanoscopic Particles. *J. Chem. Phys.* **2007**, *127*, 084703.
26. Rejman, J.; Oberle, V.; Zuhorn, I. S.; Hoekstra, D. Size-Dependent Internalization of Particles *via* the Pathways of Clathrin- and Caveolae-Mediated Endocytosis. *Biochem. J.* **2004**, *377*, 159–169.
27. Mitragotri, S.; Lahann, J. Physical Approaches to Biomaterial Design. *Nat. Mater.* **2009**, *8*, 15–23.
28. Conner, S. D.; Schmid, S. L. Regulated Portals of Entry into the Cell. *Nature* **2003**, *422*, 37–44.
29. Yue, T.; Zhang, X. Molecular Understanding of Receptor-Mediated Membrane Responses to Ligand-Coated Nanoparticles. *Soft Matter* **2011**, *7*, 9104–9112.
30. Koltover, I.; Rädler, J. O.; Safinya, C. R. Membrane Mediated Attraction and Ordered Aggregation of Colloidal Particles Bound to Giant Phospholipid Vesicles. *Phys. Rev. Lett.* **1999**, *82*, 1991–1994.
31. Reynwar, B. J.; Illya, G.; Harmandaris, V. A.; Müller, M. M.; Kremer, K.; Deserno, M. Aggregation and Vesiculation of Membrane Proteins by Curvature-Mediated Interactions. *Nature* **2007**, *447*, 461–464.
32. Reynwar, B. J.; Deserno, M. Membrane-Mediated Interactions between Circular Particles in the Strongly Curved Regime. *Soft Matter* **2011**, *7*, 8567–8575.
33. Hong, B.; Qiu, F.; Zhang, H.; Yang, Y. Budding Dynamics of Individual Domains in Multicomponent Membranes Simulated by N-Varied Dissipative Particle Dynamics. *J. Phys. Chem. B* **2007**, *111*, 5837–5849.
34. Yue, T.; Li, S.; Zhang, X.; Wang, W. The Relationship Between Membrane Curvature Generation and Clustering of Anchored Proteins: A Computer Simulation Study. *Soft Matter* **2010**, *6*, 6109–6118.
35. Kumar, P. B. S.; Gompper, G.; Lipowsky, R. Budding Dynamics of Multicomponent Membranes. *Phys. Rev. Lett.* **2001**, *86*, 3911–3914.
36. Li, S.; Zhang, X.; Wang, W. Clustering Formation of Anchored Proteins Induced by Membrane-Mediated Interaction. *Biophys. J.* **2010**, *98*, 2554–2563.
37. Venturoli, M.; Smit, B.; Sperotto, M. M. Simulation Studies of Protein-Induced Bilayer Deformations, and Lipid-Induced Protein Tilting, on a Mesoscopic Model for Lipid Bilayers with Embedded Proteins. *Biophys. J.* **2005**, *88*, 1778–1798.
38. Meyer, F. J.; Venturoli, M.; Smit, B. Molecular Simulation of Lipid-Mediated Protein-Protein Interactions. *Biophys. J.* **2008**, *95*, 1851–1865.
39. Shillcock, J. C.; Lipowsky, R. Tension-Induced Fusion of Bilayer Membranes and Vesicles. *Nat. Mater.* **2005**, *4*, 225–228.
40. Grafmüller, A.; Shillcock, J.; Lipowsky, R. Pathway of Membrane Fusion with Two Tension-Dependent Energy Barriers. *Phys. Rev. Lett.* **2007**, *98*, 218101.
41. Español, P.; Warren, P. Statistical Mechanics of Dissipative Particle Dynamics. *Europhys. Lett.* **1995**, *30*, 191–196.
42. Groot, R. D.; Warren, P. B. Dissipative Particle Dynamics: Bridging the Gap between Atomistic and Mesoscopic Simulation. *J. Chem. Phys.* **1997**, *107*, 4423–4435.
43. Hoogerbrugge, P. J.; Koelman, J. M. V. A. Simulating Microscopic Hydrodynamic Phenomena with Dissipative Particle Dynamics. *Europhys. Lett.* **1992**, *19*, 155–160.
44. Li, S.; Zhang, X.; Dong, W.; Wang, W. Computer Simulation of Solute Exchange Ssing Micelles by a Collision-Driven Fusion Process. *Langmuir* **2008**, *24*, 9344–9353.
45. Li, S.; Zheng, F.; Zhang, X.; Wang, W. Stability and Rupture of Archaebacterial Cell Membrane: A Model Study. *J. Phys. Chem. B* **2009**, *113*, 1143–1152.